Melt rheology, phase structure and impact properties of injection-moulded samples of isotactic polypropylene/ethylene–propylene copolymer (iPP/EPR) blends: influence of molecular structure of EPR copolymers

L. D'Orazio, C. Mancarella, E. Martuscelli* and G. Sticotti
Istituto di Richerche su Tecnologia dei Polimeri e Reologia del CNR, Via Toiano 6, 80072 Arco Felice, Napoli, Italy

and P. Massari
Himont SPA, Ferrara, Italy
(Received 22 December 1991; revised 4 June 1992)

Isotactic polypropylene (iPP) based blends containing as second component ethylene–propylene copolymers (EPR) having, for constant propylene (C_3) content (wt/wt), different average molecular masses ($\overline{M}_w$ and/or $\overline{M}_n$) and, for constant average molecular mass, different molecular mass distributions (*MMD*) were investigated. The study was undertaken to establish the influence of the melt phase viscosity ratio μ in determining the average particle size of the EPR phase in the vicinity of the minimum expected according to the Taylor–Tomotika theory for the average particle size *versus* $\log \mu$ function, when μ is about equal to unity (in previous studies we have in fact reached μ values far above 1). Moreoever, we also report the effects of molecular mass and molecular mass distribution of the EPR phase on the melt rheological behaviour of iPP/EPR blends, on the mode and state of dispersion of the EPR phase in the melt, as well as, in the solid state after iPP crystallization in injection moulded samples, on the crystalline lamellar thickness and the thickness of the amorphous interlayer of iPP phase, and finally on the impact properties of blend materials. It should be pointed out that the apparent viscosity of all the iPP/EPR blends investigated is expected to obey the logarithm additivity rule that applies at constant temperature and shear rate. The application of the Cross–Bueche equation revealed that the zero-shear viscosity η_0 of these iPP/EPR blends deviates positively from the logarithm additivity rule. Assuming that the crystallization of the iPP phase freezes the morphology of the EPR phase, a strict correlation is confirmed to exist between the values of EPR particle size and EPR particle size range, as measured by scanning electron microscopy on samples in the solid state, and μ value. The number average particle diameter ($\overline{D}_n$) and the particle size range of the EPR phase (D) are found to increase with increasing μ value as expected according to the Taylor–Tomotika theory. Finally, when the iPP phase crystallizes from its blends with EPR under non-isothermal conditions, the phase structure developed in the blends is characterized by lamellar thickness and interlamellar amorphous layer thickness, respectively, lower and higher than that shown by plain iPP.

(Keywords: polypropylene; ethylene–propylene random copolymers; blends; rheology; phase structure; impact properties; molecular structure)

INTRODUCTION

The results of an investigation concerned with isotactic polypropylene (iPP) based blends containing as second component ethylene–propylene copolymers (EPR) having different propylene contents (C_3) (wt/wt) and molecular-mass distributions (*MMD*) and, for fixed C_3 content and *MMD* almost constant, different average molecular masses were reported in a previous paper[1]. From such studies, aimed at establishing the influence of EPR molecular structure and composition on melt rheology, on mode and state of dispersion of the minor component in the melt, as well as, in the solid state, on impact properties of injection-moulded samples, direct correlations between molecular structure of EPR, rheological behaviour of the blend system, size of rubbery particles and impact resistance were drawn. It was found that the values of the blend zero-shear viscosity (η_0) and of a characteristic relaxation time (α(blend)) parameter, obtained by applying the Cross equation, decreased with increasing dispersion coarseness of the minor component, in agreement with results already obtained while studying a different immiscible blend system made up of polyamide-6 and ethylene–vinyl acetate copolymer[2]. The size and size distribution of EPR domains were determined from the value of the phase viscosity ratio (μ) irrespective of C_3 content along the EPR chain. The trend of the number-average particle

* To whom correspondence should be addressed

0032-3861/93/173671-11

diameter ($\overline{D_n}$) *versus* log μ showed that $\overline{D_n}$ decreased with decreasing log μ, in agreement with expectation on the basis of Taylor–Tomotika theory. Moreover, the average particle size effective for iPP toughening was found to be dependent on test temperature; for a temperature higher than the T_g of EPR and close to T_g of iPP, such an average value was, in fact, lower than that effective at room temperature.

According to Taylor–Tomotika theory the diameter of a cylindrical thread of a viscous liquid suspended in another one *versus* the logarithm of the melt-phase viscosity ratio (μ) function should show a minimum in the vicinity of $\mu = 1$. The iPP and EPR samples used in the previous study permitted us to reach μ values far above 1; thus it was impossible to verify the minimum in $\overline{D_n}$ *versus* log μ function. Therefore, to assess the effects of the melt-phase viscosity ratio when the two components have melt viscosity values close to each other, i.e. in the vicinity of the minimum expected by the theory, we blended the same sample of iPP as used in the previous work (Moplen S30G) with three other samples of EPR rubbers having, for constant C_3 content fixed at 43% (wt/wt), suitable molecular masses ($\overline{M_w}$ and $\overline{M_n}$). The previous studies showed, in fact, that up to such C_3 content the range of particle size of EPR was mainly determined by μ value. Moreover, to optimize the effects of the molecular structure of EPR phase, such copolymers had, for constant average molecular mass ($\overline{M_w}$ or $\overline{M_n}$), different molecular mass distribution (*MMD*).

In addition to what we studied in the previous work[1], the effects of C_3 content along the EPR chain higher than 43% (wt/wt) have been analysed by adding to Moplen S30G two samples of EPR having a C_3 content of 50% and 58% (wt/wt); such samples are characterized by $\overline{M_w}$ quite comparable to that shown by the EPR samples with comparatively lower C_3 content. Furthermore a small-angle X-ray scattering (SAXS) investigation concerning the possible modifications induced by the addition of EPR rubber to the intrinsic morphology of the iPP matrix has been carried out.

In the present paper we report the results of studies dealing with the rheological behaviour in the molten state at the processing temperature of this type of iPP/EPR blend, with the mode and state of dispersion of the minor component developed in the solid state, after iPP crystallization, in injection moulded samples, with the crystalline lamellar thickness and the thickness of the amorphous interlayer of the iPP phase, and with the impact behaviour of the blend materials.

The final target of the research is to formulate EPR modified iPP with enhanced and/or tailored properties by optimizing the molecular structure of the rubber.

EXPERIMENTAL

Materials

The materials used in this study were an isotactic polypropylene (iPP) made by Himont and five ethylene–propylene random copolymers (EPR) supplied by Dutral. The molecular characteristics of these polymers are summarized in *Table 1*.

Blending and sample preparation

The iPP and EPR copolymers were mixed in a Banbury mixer at 200°C with a blending time of 5 min. Blends with composition iPP/EPR 80/20 (wt/wt) were prepared. After blending, the materials were injection moulded by means of an injection press at 200°C with a mould temperature of 60°C.

Techniques

Oscillatory shearing flow properties. The oscillatory shearing flow properties, namely the complex viscosity η^* (defined by $\eta^* = \eta' - i\eta''$, where η' is the dynamic viscosity or the real part of the viscosity, η'' is the imaginary part of the viscosity and $i = \sqrt{-1}$), the storage modulus G' (defined by $G' = \omega\eta''$, where ω is the frequency of oscillation in radians per second) and the loss modulus G'' (defined by $G'' = \omega\eta'$), of the homopolymers and blends were determined at 200°C by means of a Rheometrics Mechanical Spectrometer in the plate–plate mode with an angular frequency ranging between 10^{-2} and 10^2 rad s^{-1}.

Calorimetric measurements. The glass transition temperatures T_g, the observed melting temperatures T'_m and the crystallinity index of plain iPP and its blends with EPR copolymers were obtained by using a Mettler TA 3000 differential scanning calorimeter.

The following procedure was used: the samples of plain iPP and iPP/EPR blends (about 15 mg) were heated from −100 up to 200°C at a rate of 20°C min^{-1} and the heat (dH/dt) evolved during the scanning process was recorded as a function of temperature. The T_g was taken as the temperature corresponding to 50% of the transition. The observed melting temperature T'_m and the apparent enthalpies of fusion ΔH^* were obtained from the inflection point and area of the melting peaks respectively.

Table 1 Molecular characteristics and glass transition temperatures (T_g) of neat isotactic polypropylene (iPP) and ethylene-propylene copolymers (EPR)

Sample	$\overline{M_n} \times 10^3$	$\overline{M_w} \times 10^3$	$\overline{M_z} \times 10^3$	$\overline{M_w}/\overline{M_n}$	C_3 (%wt/wt)	T_g (°C)
iPP	65	484	2782	7.4	-	−10
EPR1	40	110	300	2.8	43	−53
EPR2	70	180	500	2.8	50	−55
EPR3	73	259	860	3.5	58	-
EPR4	50	200	800	4.0	43	−49
EPR5	15	200	1000	13.3	44	−48

Molecular characteristics and glass transition temperatures (T_g) of neat isotactic polypropylene (iPP) and ethylene–propylene copolymers (EPR)

Mode and state of dispersion of minor component. The mode and state of dispersion of the minor component were investigated by means of a scanning electron microscope (Philips SEM 501). The morphological analysis was performed on fracture surfaces of blend samples broken at −40°C after coating with gold–palladium.

Small-angle X-ray scattering. Small-angle X-ray scattering (SAXS) studies were carried out on injection moulded samples of plain iPP and iPP/EPR blends by means of a compact Kratky camera equipped with a Braun one-dimensional positional detector. Ni-filtered Cu Kα radiation, generated from a Philips X-ray generator (PW 1730/10) operating at 40 kV and 30 μA, was used. The raw scattering data were corrected for parasitic scattering, absorption and slit smearing using Vonk's method[3]. The desmeared intensities were then Lorentz factor corrected[4] by multiplying by s^2 ($s = 2 \sin \vartheta/\lambda$).

Izod impact strength. Notched Izod impact strengths of the injection-moulded samples were measured by means of a Ceast pendulum in a temperature range from −40 up to 23°C according to ASTM D256. By SEM a fractographic analysis of such broken surfaces was also carried out.

RESULTS AND DISCUSSION

Melt rheology of single components and blends

Dynamic viscoelastic properties of single components and blends. The logarithms of the modulus of the complex viscosity ($|\eta^*|$), of the dynamic storage modulus (G') and of the loss modulus (G'') as functions of the logarithm of the investigated frequencies for plain iPP and EPR copolymers are reported in *Figure 1*. As shown, and as expected on the basis of results already obtained by studying different iPP and EPR samples[1], for both iPP and EPR copolymers $|\eta^*|$ values decrease, whereas G'

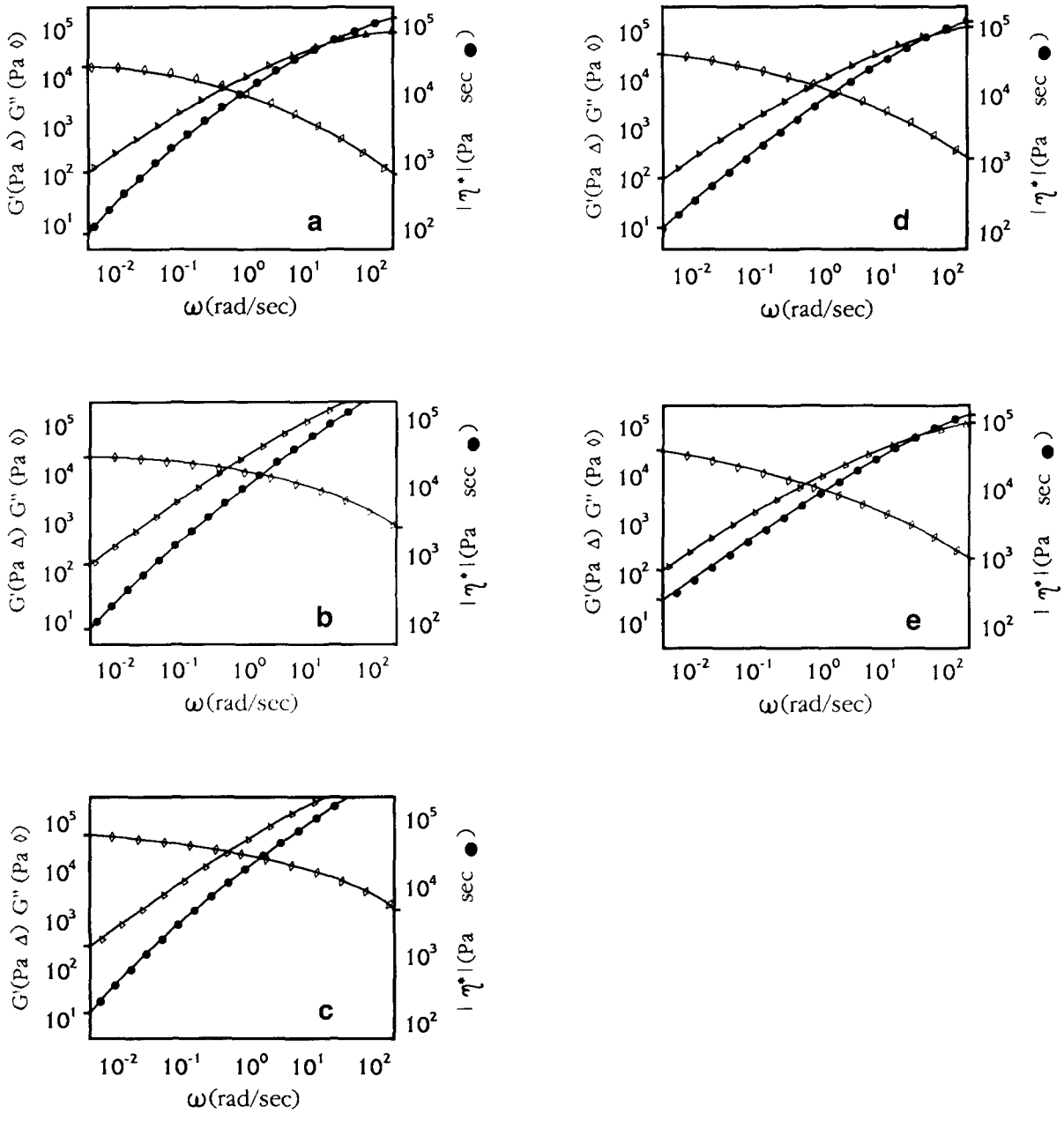

Figure 1 Logarithm of modulus value of complex viscosity ($|\eta^*|$), of dynamic storage modulus (G') and of loss modulus (G'') values as functions of logarithm of frequency for plain iPP (a), for plain EPR1 (b), for plain EPR2 (c), for plain EPR4 (d) and for plain EPR5 (e)

and G'' values increase, with increasing frequency. Note that the EPR1, EPR2 and EPR4, EPR5 samples show different rheological behaviour (compare *Figures 1b* and *1c* with *Figures 1d* and *1e* respectively). A larger reduction in viscosity with increasing frequency and G' values higher than G'' values in the last investigated decade are exhibited by the EPR4 and EPR5 samples, whereas the EPR1 and EPR2 samples show comparatively lower depression of η^* with increasing frequency and G'' values higher than G' values in the whole range of investigated frequencies (compare *Figures 1d* and *1e* with *Figures 1b* and *1c*).

Taking into account that the average molecular mass $\overline{M}_w$ dominates the viscosity at low frequency, whereas a molecular mass between $\overline{M}_n$ and $\overline{M}_w$ appears to determine the viscosity at high frequency[5–8], the finding that different rheological behaviour is shown by samples having almost the same $\overline{M}_w$ and/or $\overline{M}_n$ but different molecular-mass distribution (*MMD*) (compare the molecular characteristics of EPR2 with those of EPR5 and EPR4 in *Table 1*) indicates that the dynamic viscoelastic properties of EPR copolymers investigated are, at least in the range of explored frequencies, mainly dictated by their *MMD*. With increasing $\overline{M}_w/\overline{M}_n$ ratio, the frequency at which non-Newtonian behaviour becomes apparent shifts to lower value and the melts show a higher sensitivity to frequency, a larger decrease of η^* with increasing frequency occurring.

Finally, it should be underlined that the dynamic viscoelastic properties shown by the EPR samples characterized by broader *MMD* (EPR4 and EPR5) are comparable to that shown by plain iPP.

Figure 2 shows the typical dependence of the logarithm of the modulus value of the complex viscosity ($|\eta^*|$) upon the logarithm of the investigated frequencies for the iPP/EPR blends; for the sake of comparison, also shown in each plot are the η logarithms obtained by applying the following logarithm rule, which applies at constant temperature and shear rate[9,10]:

$$\log \eta = \Phi_1 \log \eta_1 + \Phi_2 \log \eta_2 \qquad (1)$$

where η is the viscosity of the mixture, η_1 and η_2 are the viscosities of the two components measured at the same temperature, and Φ_1 and Φ_2 are their volume fractions. As shown in *Figure 2* and as expected, iPP/EPR melts are pseudoplastic in the whole range of explored frequencies, i.e. η values decrease with increasing frequency. It is, at the same time, very surprising to find that mixing iPP and EPR copolymers results in a decrease in blend viscosity according to equation (1). Such unexpected results seem to suggest that in such iPP/EPR blends there is no mutual influence of the single components despite their melt immiscibility and heterogeneity.

The above finding disagrees with the results obtained by Danesi *et al.*[11] by means of capillary rheometer and

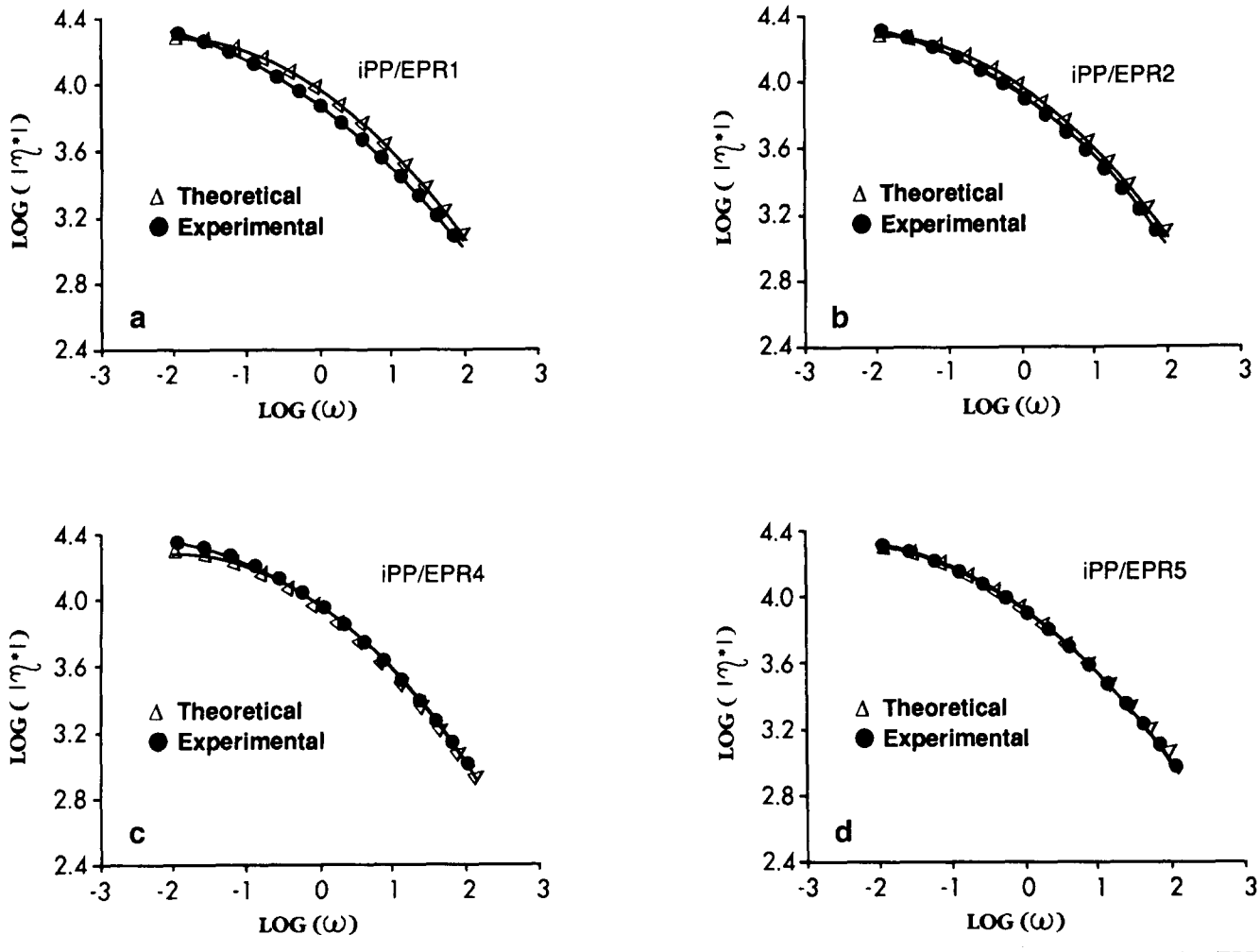

Figure 2 Dependence of logarithm of modulus value of complex viscosity ($|\eta^*|$) upon logarithm of frequency for iPP/EPR1 (a), iPP/EPR2 (b), iPP/EPR4 (c) and iPP/EPR5 (d) blends

by us[1] by means of Rheometrix on samples of blends containing the same iPP, but different EPR copolymers, showing that iPP/EPR blends are to be classified as negative deviation blends (NDB), i.e. the blend viscosity decreases below the mean value of the viscosities of the two plain components. Taking into account that the EPR copolymers used in this work have viscosity lower than those previously used and close enough to iPP viscosity, the conflict between the results suggests that very different rheological behaviours can be exhibited by iPP/EPR blends depending on the molecular structure of EPR rubber component, i.e. depending on the melt-phase viscosity ratio.

The dependence of the logarithm of the elastic modulus G' and the loss modulus G'' upon the logarithm of the investigated frequencies of the iPP/EPR blends are shown in *Figures 3* and *4*. It is to be noted that, in agreement with the results already obtained[1], all the iPP/EPR blends show the same G' and G'' values in the whole range of explored frequencies. At low frequency the blends containing the EPR copolymers with narrower *MMD* (EPR1 and EPR2) exhibit G' values slightly higher than that of the single components, whereas the blends containing the EPR copolymers with broader *MMD* show G' values intermediate between that of the single components (compare *Figure 3a* with *Figure 3b*). Such findings could suggest that, in the first investigated decade, the amount of energy stored by a blend system depends on the *MMD* of EPR and tends to increase on decreasing the $\overline{M_w}/\overline{M_n}$ ratio.

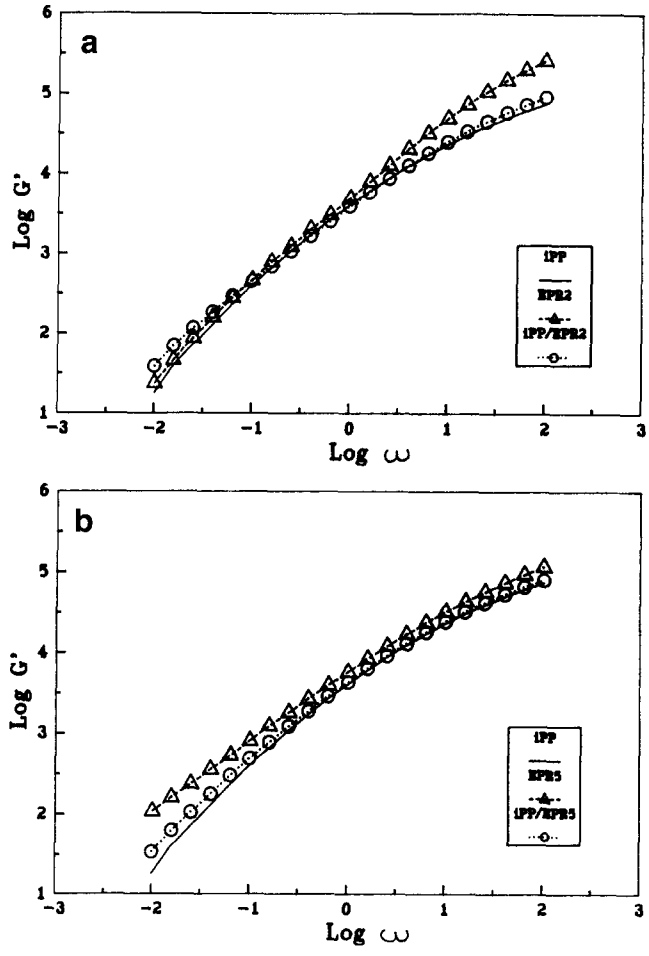

Figure 3 Dependence of logarithm of elastic modulus values (G') upon logarithm of frequency for iPP/EPR2 blend (a) and iPP/EPR5 (b)

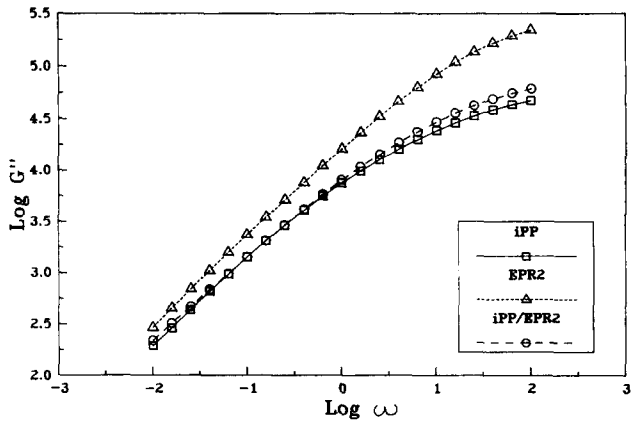

Figure 4 Dependence of logarithm of loss modulus (G'') upon logarithm of frequency for iPP/EPR2 blend

Table 2 Application of Cross–Bueche equation to plain iPP and EPR copolymers and to iPP/EPR blends: values of zero shear viscosity (η_0), characteristic relaxation time (α) and m; the zero shear viscosity values calculated assuming log addivity rule for iPP/EPR blends (η'_0) are also reported

Sample	η_0 (P)	α (s)	m	η'_0 (P)
iPP	164 100	0.722	2/3	–
EPR1	218 390	0.267	4/7	–
EPR2	271 000	0.281	4/7	–
EPR4	331 016	1.735	4/7	–
EPR5	307 500	1.761	4/7	–
iPP/EPR1	188 000	1.110	4/7	174 053
iPP/EPR2	221 141	1.050	4/7	181 967
iPP/EPR3	171 615	1.089	4/7	–
iPP/EPR4	287 356	1.143	4/7	189 622
iPP/EPR5	263 300	1.152	4/7	186 765

With increasing frequency the G' values shown by all the iPP/EPR blends investigated approach that shown by plain iPP.

In the whole range of explored frequencies the amount of energy dissipated by all the iPP/EPR blends is substantially the same as that dissipated by plan iPP, in agreement with our previous results[1].

Determination of zero-shear viscosity of single components and blends. Taking into account that in oscillatory measurements on polymer melts the frequency (ω) becomes analogous to shear rate ($\dot{\gamma}$)[12–15] and assuming an approximate equivalence of $|\eta^*|$ and apparent viscosity (η_a)[15–20], the zero-shear viscosity (η_0) of both single components and blends was calculated by using the following modified Cross–Bueche equation[21]:

$$\eta_0\eta_a = 1 + (\alpha\dot{\gamma})^m \qquad (2)$$

where η_0 is the zero-shear viscosity, α is a parameter that according to Cross should correspond to the characteristic relaxation time related to molecular mass for the linear polymer solution and m gives a measure of the shear thinning of the melt. According to Iwakura *et al.*[22] for polymer melts α is related to the size of the apparent flow unit; the reciprocal of α corresponds to the shear rate at which $\eta_a = \eta_0/2$. The m values found for the single components to obtain linearity in plots of $1/\eta_a$ *versus* $\dot{\gamma}^m$ are reported in *Table 2*. As shown for plain iPP m assumes the value usually obtained for a polymer with

a MMD (2/3)[21]; whereas for the EPR copolymers m values are lower (4/7), indicating a less severe shear thinning in the non-Newtonian region.

From the lines $1/\eta_a$ *versus* $\dot{\gamma}^m$ the zero-shear viscosity η_0 and α are easily obtained from the reciprocal of the intercept and from the slope respectively. The η_0 and α values of the plain iPP and EPR copolymers are also listed in *Table 2*. As shown, the plain iPP at 200°C has a zero-shear viscosity lower than that of the pure EPR rubbers and the η_0 values shown by the EPR copolymers are proportional to an average molecular mass greater than $\overline{M}_w$, likely between $\overline{M}_w$ and $\overline{M}_z$ (see *Table 1*). As far as α values are concerned, the plain iPP shows a relaxation time longer than that shown by EPR1 and EPR2 samples and shorter than that shown by EPR4 and EPR5 samples. As the reciprocal of the parameter α corresponds to the shear rate at which η_a decreases to half of η_0, shorter α values means that non-Newtonian flow starts at larger shear rate. Thus the range of Newtonian behaviour of plain iPP is expected to be smaller than that of EPR1 and EPR2 copolymers and larger than that of EPR4 and EPR5 copolymers.

The m, η_0 and α values calculated for iPP/EPR blends are reported in *Table 2*; the zero-shear viscosity values for the blends obtained assuming the additivity logarithm rule (η'_0) are also reported. As shown for all investigated blends the m parameter assumes the value of 4/7, suggesting that the blend system undergoes a shear thinning less severe than that of plain iPP in the non-Newtonian region. It is to be noted that these iPP/EPR blends, as far as η_0 is concerned, show a positive deviation from the logarithm additivity rule. Moreover, the extent of such a deviation increases on increasing the EPR average molecular mass ($\overline{M}_w$ or likely an average molecular mass between $\overline{M}_w$ and $\overline{M}_z$). Such a result disagrees with that obtained in the previous work[1], showing η_0(blend) values with a large negative deviation from equation (1).

The α values shown by all investigated blends are comparable to each other; such values are longer than that shown by plain iPP, indicating that, in these blend systems, the transition from Newtonian to pseudoplastic flow starts at a frequency lower than that of plain iPP; an opposite result was obtained in the previous work[1].

The different rheological behaviours shown by the iPP/EPR blends studied in the present work, also in the absence of shear, are presumably related to the fact that for such blends the range of phase viscosity ratio (μ), defined as the ratio between the zero shear viscosity of the amorphous polymer phase (η_0^a) and the zero shear viscosity of the crystallizable polymer phase (η_0^c), tends closely to approach unity (see *Table 4*). In the absence of shear it could be supposed that the system may be described in terms of a continuous two-phase model, where the macromolecules of one phase are physically entrapped into the macromolecules of the other phase.

Thermal behaviour and crystallinity

The glass transition temperatures (T_g) shown by the plain iPP and EPR copolymers are listed in *Table 1*. The apparent melting temperatures (T'_m) of plain iPP and of iPP crystallized from its blends and the crystallinity index of iPP/EPR blends (X_c(blend)) and of iPP phase (X_c(iPP)) are reported in *Table 3*. As shown and as expected, the iPP T_g lies around −10°C and the EPR T_g are located in the range −48 to −55°C. Note that among EPR samples comparatively lower T_g is shown by the samples having narrower MMD (EPR1 and EPR2).

Table 3 Apparent melting temperatures (T'_m) of plain iPP and iPP/EPR blends and crystallinity index of the plain iPP and iPP crystallized from its blends with EPR copolymers

Sample	T'_m (°C)	X_c(blend)	X_c(iPP)
iPP	169	37	37
iPP/EPR1	166	29	36
iPP/EPR2	167	31	38
iPP/EPR3	167	28	36
iPP/EPR4	168	29	36
iPP/EPR5	166	30	38

The d.s.c. thermograms of the injection moulded samples of the iPP/EPR blends show two distinct glass transition temperatures (T_g) and a single endothermic peak when heated from −100 to 200°C. The T_g at lower temperature corresponds to T_g of EPR phase, while that at higher temperature to T_g of iPP phase; such a finding confirms that, also in the amorphous condensed phase, there is no miscibility between the two components.

The temperature position of the endothermic peaks (T'_m), reported in *Table 3*, is characteristic of the melting of the α-crystalline form of iPP. The apparent melting temperatures shown by iPP crystallized from its blends with EPR copolymers are slightly lower than that of plain iPP, irrespective of the EPR molecular structure. Such a finding indicates that the melting behaviour of the iPP is to be considered independent of EPR and EPR molecular structure; the perfection and thickness of the growing iPP crystals are almost unaffected by the presence of the EPR rubbery phase, irrespective of its molecular characteristics. Thus, according to previous results[21] iPP and EPR are confirmed to be immiscible in the molten state.

The X_c(blend) values are lower than that of plain iPP, and the X_c(iPP) values shown by the iPP phase crystallized in the presence of EPR phase strictly approach that exhibited by the neat iPP phase with no dependence on EPR molecular structure (see *Table 5*). Such findings, contrary to what was found while studying isothermally crystallized samples of different iPP/EPR blends[23], indicate that when iPP crystallizes from its blends with EPR in non-isothermal conditions the rubbery component does not interfere with the crystallization process.

Phase structure

Mode and state of dispersion of the minor component. The analysis by SEM of the mode and state of EPR dispersion, generated in the iPP/EPR injection moulded samples, shows that in all investigated specimens a layered structure developed in the direction perpendicular to the mould flow direction, according to the schematic model reported in *Figure 5*. As shown in *Figure 5*, on moving from the border towards the core of the sample three different layers are found:

(1) a *skin surface* (S) where no domains of EPR dispersed phase can be observed. The thickness of such a layer ranges between 15 and 20 μm, a higher skin thickness (40 μm) being shown only by the blend sample containing the EPR4 copolymer.

(2) an *intermediate transition layer* (I) where the concentration of the EPR domains increases on going

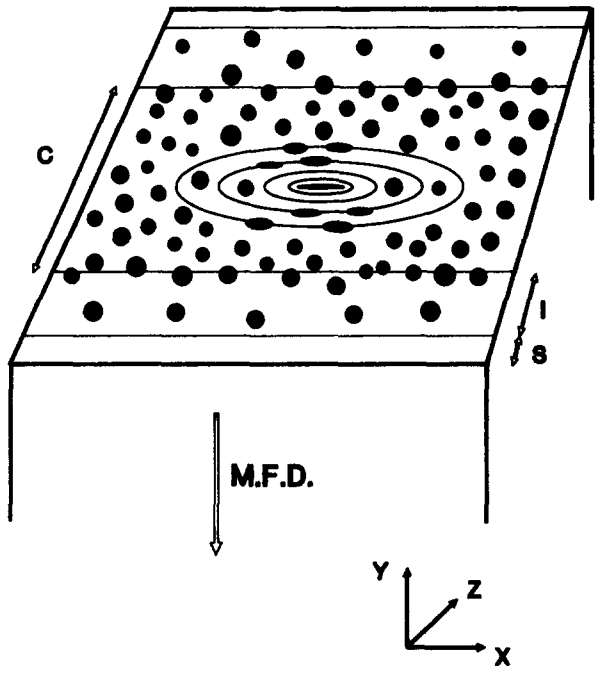

Figure 5 Schematic model of layered structure generated in iPP/EPR injection moulded samples

Table 4 Range of particle size, number average particle diameter ($\overline{D_n}$) and phase viscosity ratio (μ) for iPP/EPR blends

Sample	Range of particle size (μm)	$\overline{D_n}$ (μm)	μ
iPP/EPR1	0.1–0.4	0.25	1.33
iPP/EPR2	0.1–0.5	0.30	1.65
iPP/EPR3	0.1–0.4	0.25	–
iPP/EPR4	0.1–0.6	0.35	2.02
iPP/EPR5	0.4–1.2	0.80	1.87

towards the core of the samples with gradient characteristic. The thickness of such a layer ranges between 20 and 25 μm, only blend sample with EPR4 copolymer showing a comparatively higher thickness (40 μm).

Taking into account that, generally, in flowing systems of two immiscible polymers the low viscosity component tends to become the continuous phase and to encapsulate the high viscosity component, the findings that the sample with EPR4 copolymer exhibits comparatively higher thickness of both skin and intermediate transition layers are to be related to the comparatively higher μ value calculated for the iPP/EPR4 blend, showing that the zero-shear viscosity of the plain iPP is twice as low as that of the EPR copolymer (see *Table 4*).

(3) a *core* (C) showing an EPR droplet-like morphology. The range of diameters of the EPR particles is reported in *Table 4* together with the number average of such diameters ($\overline{D_n}$) and the μ value of the blends. As shown, with the exclusion of the blend containing the EPR5 copolymer, the range of particle size and the average particle size of the dispersed phase are determined by the μ value; those quantities increasing with μ. Analogous conclusions were already drawn while studying blends based on the same iPP with different EPR copolymers[1]. The trend of the $\overline{D_n}$ values *versus* $\log\mu$ shows that $\overline{D_n}$ decreases with decreasing $\log\mu$ (see *Table 4* and *Figure 6*) in agreement with the expectation on the basis of the Rayleigh–Taylor–Tomotika theory[24–27]. The finding that the average size shown by the blend containing the EPR5 copolymer does not agree with the prediction of Taylor–Tomotika theory is presumably to be ascribed to the larger *MMD* exhibited by such a rubbery phase, which causes a coarser dispersion of the minor component with a broader particle size distribution.

Moreover, the transverse surfaces of all investigated blend samples show, in the direction perpendicular to the mould flow direction, concentric elliptical lines having the centre of their axis coincident with that of the samples. Such lines represent the profiles of the flow rate, frozen because of fast cooling. It should be noted that along such lines the EPR spherical-shaped domains tend to be more or less deformed assuming an ellipsoidal shape with the major axis oriented in the direction perpendicular to the mould flow direction (see *Figure 5*).

Super-reticular parameters of iPP. Typical Lorentz corrected desmeared patterns for the neat iPP and iPP/EPR blends are shown in *Figure 7*. As shown, both desmeared SAXS profiles exhibit defined maxima. By applying Bragg's law, long periods (L), calculated from the peak position, were obtained for all investigated

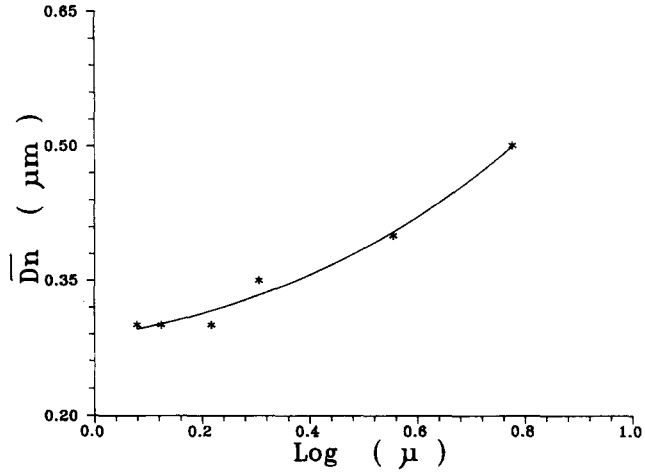

Figure 6 Plot of the number average particle size ($\overline{D_n}$) *versus* logarithm of the melt phase viscosity ratio (μ) for all investigated iPP/EPR blends

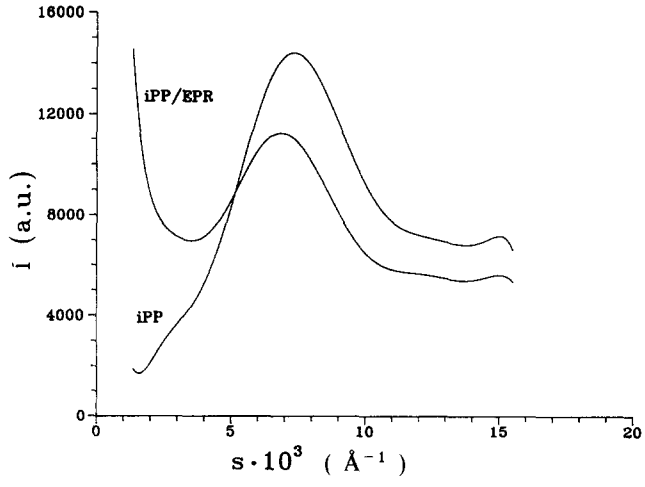

Figure 7 Typical desmeared SAXS pattern for the plain iPP and iPP/EPR blends

samples. Assuming for the iPP spherulite fibrillae a two phase model, consisting of alternating parallel crystalline lamellae and amorphous layers, from the L values the crystalline lamella thickness (L_c) was calculated by using the following relation:

$$L_c = \frac{X_c(\text{iPP})L}{(\rho_c/\rho_a)[1-X_c(\text{iPP})]-X_c(\text{iPP})} \quad (3)$$

where X_c(iPP) is the d.s.c. crystallinity index of the iPP phase, and ρ_c and ρ_a are the densities of the crystalline and amorphous iPP phase, respectively. Subtracting the obtained L_c values from the L values, the average thickness of the amorphous interlamellar layer (L_a) was obtained. In this calculation, in agreement with what was found by SEM analysis, the rubbery domains were assumed to be located in interfibrillar regions. Thus the crystallinity of iPP phase (X_c(iPP)) was considered and not that of the blend.

The L, L_c and L_a values of plain iPP (L(iPP), L_c(iPP) and L_a(iPP)) and of iPP crystallized from its blends with EPR copolymers (L(iPP/EPR), L_c(iPP/EPR) and L_a(iPP/EPR)) are reported in *Table 5*. As shown, the L(iPP) and L(iPP/EPR) values, within the experimental error (±5 Å), show no dependence on EPR molecular structure and composition. Such a finding is in agreement with results already obtained while studying isothermally crystallized samples of different iPP/EPR blends[23].

It is interesting to underline that the thickness of the crystalline lamella of iPP crystallized from its blends tends to decrease, whereas the thickness of the amorphous interlamellar layer increases (see *Table 5*). Thus when iPP crystallizes in the presence of EPR copolymers in non-isothermal conditions, the phase structure developed in the blends is characterized by lamellar thickness and interlamellar amorphous layer, respectively, lower and higher than that shown by plain iPP. Such morphological results agree with those obtained while studying isothermally crystallized samples of different iPP/EPR blends[23]. In order to explain these results, we assumed that EPR molecules with low molecular masses, because of their higher mobility, diffuse into the iPP interlamellar amorphous layer where they may form domains more or less interconnected with the amorphous iPP phase, thus increasing its thickness and hindering the iPP crystal growth.

Impact behaviour

The notched Izod impact strength values for the plain iPP and the iPP/EPR blends investigated are reported in *Figure 8* as functions of test temperatures. As expected, the plain iPP shows very poor impact properties in the whole range of explored temperatures and, for test temperature below the glass transition temperature (T_g)

Table 5 Long period (L), crystalline lamella thickness (L_c) and amorphous interlammelar layer (L_a) of the plain iPP and iPP crystallized from its blends with EPR copolymers

Sample	L (Å)	L_c (Å)	L_a (Å)
iPP	161	56	105
iPP/EPR1	168	45	123
iPP/EPR2	163	47	116
iPP/EPR3	174	45	129
iPP/EPR4	166	45	121
iPP/EPR5	172	48	124

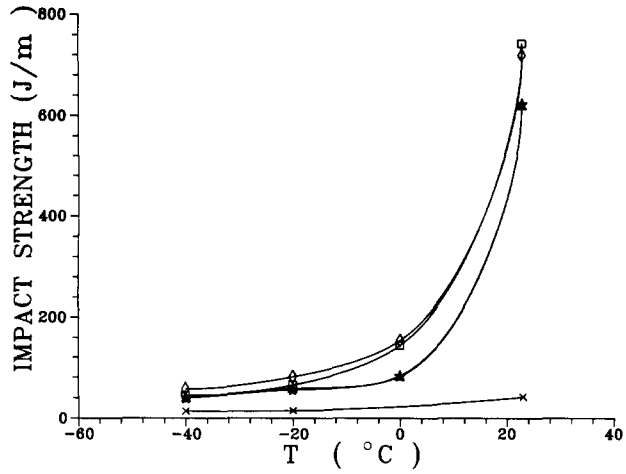

Figure 8 Notched Izod impact strength as a function of temperature for plain iPP and iPP/EPR blends: (×) iPP, (△) iPP/EPR1, (◇) iPP/EPR2, (□) iPP/EPR4, (★) iPP/EPR5

of the EPR copolymers (−40°C), no improvement in the iPP impact strength is obtained, irrespective of EPR molecular characteristics (see *Figure 8*). Such a result agrees quite well with that obtained while studying different iPP/EPR blends[1].

It is interesting to underline that, for test temperatures ranging between −40 and −20°C, the fracture surfaces of the plain iPP and of the iPP/EPR4 blend show no stress-whitening phenomenon, whereas the fracture surfaces of all the remaining blend samples, except the skin layer made of plain iPP, are more or less whitened. Particularly, the surfaces of the blend samples containing the EPR1 and EPR3 copolymers are completely whitened; those of the blend samples containing the EPR2 and EPR5 copolymers show only slight whitening localized in the sample core.

Taking into account that, for a test temperature of −40°C, iPP/EPR blend materials show no improved strength, the stress whitening phenomenon is mainly to be associated with cavitation during the test and/or a possible orientation contribution.

The fractographic analysis of the broken surfaces of plain iPP and of iPP/EPR blends shows that all samples at −40°C, as expected, break in a brittle fashion; the fracture surfaces show a crack path where practically no matrix yielding takes place. Moreover, the broken samples of plain iPP show no fracture induction area, whereas such an area, localized in the central part of the notch front, is observed in all blend samples. The size of the fracture induction area is different, with no systematic dependence on EPR molecular structure, the smallest and largest area being shown respectively by the blend sample containing the EPR4 and EPR2 copolymers (see *Figure 9*).

For test temperature higher than EPR T_g and close to iPP T_g (−10 to 0°C), enhancement in iPP impact behaviour results, dependent on the type of EPR dispersed phase (see *Figure 8*). As shown in *Figure 8* at the temperature of 0°C, higher impact strength values are shown by the blend samples containing the EPR2 and EPR4 copolymers; the same comparatively lower values are exhibited by all the remaining blend samples.

The surfaces fractured at 0°C of the blend samples containing EPR1 and EPR3 copolymers are completely whitened, whereas the fracture surfaces of all the

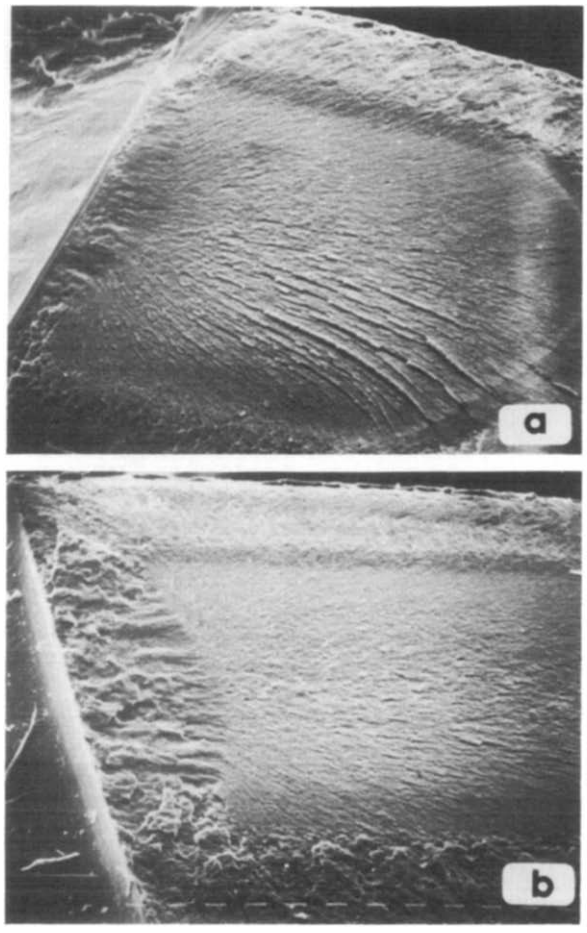

Figure 9 SEM micrographs of fracture surfaces broken at −40°C of iPP/EPR4 (a) and iPP/EPR2 (b) blends

remaining blend samples exhibit whitening localized only at the fracture induction area, and/or at the boundary between the iPP skin and the intermediate transition layer according to *Figure 5*. It is interesting to underline that better impact properties, for test temperature of 0°C, are shown by the blend samples that undergo stress whitening with lowest intensity (blend with EPR4 and EPR2 copolymers). Such a finding supports the suggestion that, at 0°C, a cavitation process, rather than multicraze formation, is associated with the observed whitening. Therefore it can be supposed that, for test temperature approaching the iPP T_g, the observed improvement in impact strength shown by the blend material could be due to yielding of the matrix.

The fractographic analysis of the surfaces of the blend sample broken at 0°C reveals that the size of the fracture induction area, where the material breaks in ductile fashion, depends on the type of EPR copolymer used. As shown in *Figure 10*, the smallest and largest induction areas are observed in the blend samples containing the EPR1 and the EPR2, EPR4 copolymers, respectively. The blend samples containing the EPR3 and EPR5 copolymers show fracture induction area with comparable intermediate size (see *Figure 10*). As expected, the best impact properties are shown by the materials that at 0°C show largest fracture induction area (blends with EPR4 and EPR2 copolymers).

The very different behaviours of such EPR copolymers as impact modifiers is reasonably ascribed to the fact that in blends with iPP they give rise to domains with different degrees of dispersion (average particle size) (see *Table 4*). It is likely that EPR particles ranging in size between 0.30 and 0.35 μm are more effective for iPP toughening, and/or in iPP/EPR4 and iPP/EPR2 blends a more effective interparticle distance is achieved, according to Wu[28]. Such values of $\overline{D_n}$, able to optimize the impact strength of iPP at 0°C, agree with that found in the previous work[1].

For test temperatures close to room temperature, the impact strength shown by the blend samples containing the EPR2 and EPR4 copolymers is higher than that shown by the remaining blend samples. With increasing test temperature, the intensity of the stress whitening phenomenon and the volume of material involved increase strongly, with no dependence on EPR type. Such a finding could suggest that, on increasing test temperature, also multicraze formation may occur. Therefore the fracture mechanism active, for test temperature close to room temperature, could result in a combination of shear yielding and multicraze formation.

CONCLUDING REMARKS

A study aimed at assessing the influence of the melt-phase viscosity ratio (μ) in determining the average particle size of EPR phase dispersed into iPP matrix in the vicinity of the minimum expected according to the Taylor–Tomotika theory for the average particle size *versus* $\log \mu$ function has been reported. Moreover the effects of the molecular masses ($\overline{M_w}$ and $\overline{M_n}$) and molecular mass distribution (*MMD*) of EPR phase on melt rheological behaviour of iPP/EPR blends on mode and state of dispersion of EPR phase in the melt, as well as, in the solid state, on intrinsic phase structure of iPP crystalline phase and on impact properties of injection moulded samples of blend materials were reported.

It should be pointed out that the apparent viscosity of all the iPP/EPR blends investigated can be expected to conform to the logarithm additivity rule that applies at constant temperature and shear rate[9], indicating that in the melt there is no mutual influence of the single components despite their immiscibility and heterogeneity. Opposite results were obtained in previous work[1] and by Danesi *et al.*[11], showing that iPP/EPR blends are to be classified as 'negative deviation blends' (NDB). Taking into account that the EPR copolymers used in this work have melt viscosity considerably lower than that of EPR copolymers previously used and quite close to the melt viscosity of the iPP, the conflict between the results suggests that the iPP/EPR blends can exhibit very different rheological behaviours depending on the molecular characteristics of the EPR rubbery component, i.e. depending on the melt phase viscosity ratio defined as the ratio between the zero shear viscosity of the amorphous polymer phase and the zero shear viscosity of the crystallizable polymer phase.

The application of the Cross–Bueche equation revealed, moreover, that the zero-shear viscosity (η_0) of these iPP/EPR blends deviates positively from the logarithm additivity rule (η'_0) and that the transition from Newtonian to pseudoplastic flow starts at a frequency lower than that of plain iPP. These results are opposite to that found in previous work[1] and support the hypothesis that in the absence of shear the melt-phase viscosity ratio (μ) is the main factor in determining the

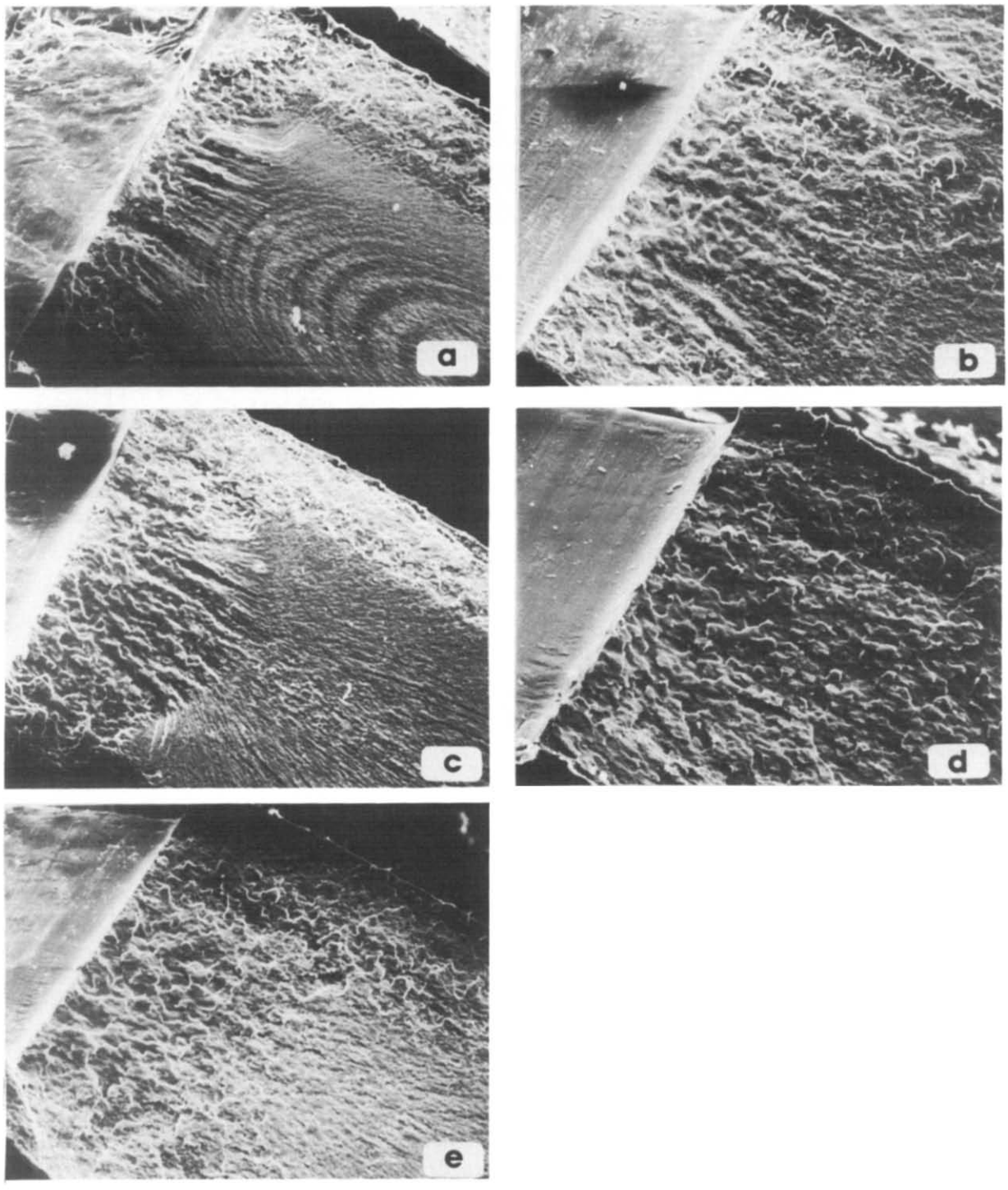

Figure 10 SEM micrographs of fracture surfaces broken at 0°C of iPP/EPR1 (a), iPP/EPR2 (b), iPP/EPR3 (c), iPP/EPR4 (d) and iPP/EPR5 (e) blends

viscosity of the blend system and its viscoelastic parameters.

Assuming that the crystallization process of iPP phase freezes the morphology of the EPR phase, a strict correlation is confirmed to exist between the values of the EPR particle size and EPR particle size range, as measured by SEM on samples in the solid state, and μ value. The number average particle diameter ($\overline{D}_n$) and the particle size range of the EPR phase (D) are found to increase with increasing μ value, with the exception of the EPR copolymer characterized by the comparatively broadest MMD (13.5). Such results, expected according to the Rayleigh–Taylor–Tomotika theory, are in agreement with that found in previous work[1].

Recall that the injection moulding process induces an anisotropic distribution of EPR dispersed phase in the direction perpendicular to the mould flow direction. Moving from the border towards the core of the samples, three different layers are found:

(1) a skin surface 15–20 μm thick, where no domains of EPR phase can be observed;

(2) an intermediate transition layer where the concentration of the EPR particles increases on going

towards the core of the sample with gradient characteristic; and

(3) a core showing an EPR droplet-like morphology, droplet size being determined according to μ value in all investigated samples except the sample containing the EPR5 copolymer. This exception to the rule is reasonably ascribed to the very large *MMD* (13.5) shown by this copolymer and to the consequent broad particle size distribution.

Moreover, when iPP phase crystallizes from its blends with EPR phase in non-isothermal conditions, the intrinsic morphology of iPP matrix is modified by the addition of rubbery component. Therefore the phase structure developed in the blends is characterized by lamellar thickness and interlamellar amorphous layer respectively lower and higher than that shown by plain iPP.

The value of $\overline{D_n}$ able to optimize the impact strength of the iPP in the temperature range of 0–20°C was confirmed to be 0.30–0.35 μm, in agreement with that found in previous work[1]. Finally it is interesting to underline that, because of the strict correlations found between the impact strength and $\overline{D_n}$ value and between $\overline{D_n}$ value and μ value, the impact behaviour of the iPP, for a given test temperature, can be directly predicted according to the value of the melt-phase viscosity ratio.

REFERENCES

1 D'Orazio, L., Mancarella, C., Martuscelli, E. and Polato, F. *Polymer* 1991, **32**, 1186
2 Addonizio, M. L., D'Orazio, L., Mancarella, C. and Martuscelli, E. *J. Mater. Sci.* 1989, **24**, 2939
3 Vonk, C. G. *J. Appl. Crystallogr.* 1975, **8**, 340
4 Alexander, L. E. 'X-Ray Diffraction in Polymer Science', Wiley, New York, 1969
5 Ballman, R. L. and Simon, R. H. M. *J. Polym. Sci. (A)* 1964, **2**, 3557
6 Ballman, R. L. *Nature* 1964, **202**, 288
7 Graessley, W. W., Hazelton, R. L. and Lindeman, L. R. *Trans. Soc. Rheol.* 1967, **11**, 267
8 Graessley, W. W. 'Advances in Polymer Science', Vol. 16, Springer-Verlag, Berlin, 1974
9 Lee, B. L. and White, J. L. *Trans. Soc. Rheol.* 1975, **19**, 481
10 Utraki, C. A. and Kamal, M. R. *Polym. Eng. Sci.* 1982, **22**, 96
11 Danesi, S. and Porter, R. S. *Polymer* 1978, **19**, 668
12 Nielsen, L. E. 'Polymer Rheology', Marcel Dekker, New York, 1977
13 Han, C. D. *J. Appl. Polym. Sci.* 1986, **32**, 3809
14 Han, C. D. *J. Appl. Polym. Sci.* 1988, **35**, 167
15 Ferry, J. D. 'Viscoelastic Properties of Polymers', 2nd Edn., Wiley, New York, 1970
16 Nielsen, L. E. 'Mechanical Properties of Polymers and Composites', Vol. 1, Marcel Dekker, New York, 1974
17 Cox, W. P. and Merz, E. H. *J. Polym. Sci.* 1958, **28**, 619
18 Onogi, S., Masuda, T. and Ibaragi, T. *Kolloid Z.* 1968, **222**, 110
19 Onogi, S., Fujii, T., Kato, H. and Ogihara, S. *J. Phys. Chem.* 1964, **68**, 1598
20 Verser, D. W. and Maxwell, B. *Polym. Eng. Sci.* 1970, **10**, 122
21 Cross, M. M. *J. Appl. Polym. Sci.* 1969, **13**, 765
22 Iwakura, K. and Fujimura, T. *J. Appl. Polym. Sci.* 1975, **19**, 1427
23 D'Orazio, L., Mancarella, C., Martuscelli, E. and Sticotti, G. *J. Mater. Sci.* 1991, **26**, 4033
24 Rayleigh, J. W. S. *Proc. R. Soc.* 1879, **29**, 71
25 Taylor, G. *Proc. R. Soc. (A)* 1934, **146**, 501
26 Tomotika, S. *Proc. R. Soc. (A)* 1935, **150**, 322
27 Tomotika, S. *Proc. R. Soc. (A)* 1936, **153**, 308
28 Wu, S. *Polymer* 1985, **26**, 1855